Multispectral Imaging and Convolutional Neural Network for Photosynthetic Pigments Prediction

Kestrilia R. Prilianti
Informatics Engineering Department
Universitas Ma Chung
Malang, Indonesia
kestrilia.rega@machung.ac.id

Ivan C. Onggara
Informatics Engineering Department
Universitas Ma Chung
Malang, Indonesia

Marcelinus A.S. Adhiwibawa
Ma Chung Research Center for
Photosynthetic Pigments (MRCPP)
Malang, Indonesia
marcelinus.setya@machung.ac.id

Tatas H.P. Brotosudarmo
Ma Chung Research Center for
Photosynthetic Pigments (MRCPP)
Malang, Indonesia
tatas.brotosudarmo@machung.ac.id

Syaiful Anam
Mathematics Department
Universitas Brawijaya
Malang, Indonesia
syaiful@ub.ac.id

Agus Suryanto
Mathematics Department
Universitas Brawijaya
Malang, Indonesia
suryanto@ub.ac.id

Abstract—**The evaluation of photosynthetic pigments composition is an essential task in agricultural studies. This is due to the fact that pigments composition could well represent the plant characteristics such as age and varieties. It could also describe the plant conditions, for example, nutrient deficiency, senescence, and responses under stress. Pigment role as light absorber makes it visually colorful. This colorful appearance provides benefits to the researcher on conducting a non-destructive analysis through a plant color digital image. In this research, a multispectral digital image was used to analyze three main photosynthetic pigments, i.e., chlorophyll, carotenoid, and anthocyanin in a plant leaf. Moreover, Convolutional Neural Network (CNN) model was developed to deliver a real-time analysis system. Input of the system is a plant leaf multispectral digital image, and the output is a content prediction of the pigments. It is proven that the CNN model could well recognize the relationship pattern between leaf digital image and pigments content. The best CNN architecture was found on *ShallowNet* model using Adaptive Moment Estimation (Adam) optimizer, batch size 30 and trained with 15 epoch. It performs satisfying prediction with MSE 0.0037 for in sample and 0.0060 for out sample prediction (actual data range -0.1 up to 2.2).**

Keywords—convolutional neural network, multispectral digital image, non-destructive evaluation, photosynthetic pigments

I. INTRODUCTION

Knowledge about photosynthetic pigments composition in a plant is essential due to its vital role in plant development stages. The pigments composition alteration is also known strongly represent the plant responses to internal factors and environmental changes [1]. Therefore, studies to develop an efficient method to describe pigment composition within the plant is one among the important topics in agriculture.

As digital technology is proliferating, a nowadays efficient way in plant evaluation is commonly related to the concept of real time and non-destructive measurement [2]. Digital imaging together with artificial intelligence now become a popular methods to conduct a real-time and non-destructive evaluation [3]. It is now possible to determine and quantify pigments within the plant through its digital image. Moreover, much valuable information could be provided automatically by implementing artificial intelligence method on those quantifications. Such approaches are proven significantly more efficient in cost and time.

Artificial neural network (ANN) is widely used by the agricultural researchers to conduct classification and

prediction on a plant. Some tasks are known to use ANN as the primary data analysis method, e.g, leaf area estimation [4], yield prediction [5], fruit weight prediction [6], leaf chlorophyll prediction [7], and leaf classification [8]. Plant digital image was used as raw data on most of those tasks. Prior to the learning process, the feature extraction step of the digital image must be done. For example: (1) Reference [7] created 19 features from red, green, blue components of RGB color space and hue, saturation, intensity components of HSI color space; (2) Reference [8] used 13 morphological features such as number of boundary pixel, geometric center, number of pixels of the object, etc. Indeed, the accuracy of the ANN model highly depends on the ability of the researcher to determine or create the best features. Therefore, study about feature extraction is one of the critical tasks in developing an ANN model with a digital image as the raw data. Regarding this difficulties, deep learning was created to automate the feature extraction process. It reduces the system dependency on the prior human knowledge and minimizes the human effort to design the feature [9].

Convolutional Neural Network (CNN) is one of the most popular architectures of deep learning. The convolutional term is taken from the morphological image processing technique. Convolutional matrix is applied on an image for edge detection, blurring, sharpening, embossing, and more. In CNN algorithm, convolution is the primary process for each layer. Many CNN projects were aimed to classify digital image based on the object shape. However, some researcher proved that CNN is also superior to classify digital image based on the object color [10,11]. Some CCN projects on plant image are species classification [12,13], phenotyping [14] and disease detection [15]. In this research, CNN was used as the main tools to determine and quantify the pigments contained in the plant to create a novel non-destructive photosynthetic pigments prediction system. The system's input is a multispectral digital image of a plant leaf, and the output is the prediction of three main photosynthetic pigments content. Those pigments are chlorophyll, carotenoid, and anthocyanin. Data of the actual pigment content were provided by conducting spectrophotometry on the plant leaf which the picture was taken by digital camera. Those data were used to train the CNN architecture. Three CNN models with different level of complexity were evaluated to determine the most suitable architecture for pigments content prediction. Moreover, two different optimizers were also compared to acquire the best result.

II. MATERIALS AND METHODS

A. Sample Preparation

Syzygium oleana and *Piper betle L* leaves were used in the experiment. Variation of carotenoid content was provided by the yellowish *Piper betle L* leaves, and variation of anthocyanin content was provided by the reddish *Syzygium oleana* leaves. There were as much as 444 leaves prepared for the data collection. Each leaf was chosen with the consideration of data variation fulfillment. Color variation, age, and position from the terminal bud were among the contemplations. This is vital concerning that the CNN learning process will rely upon it. Samples were divided into two sets, a training set, and a test set. The training set was used by the CNN architecture to learn the data and create the relationship model whereas the test set was used to evaluate the prediction performance of the model. Each sample will go through two data acquisition process. The first is multispectral digital image acquisition using a digital camera. The other data acquisition was laboratory analysis to identify and measure the pigments contained in each leaf using Spectrophotometry method.

B. Multispectral Image Acquisition

Photosynthetic pigments only absorb light at a specific wavelength and reflecting others [16], e.g., chlorophyll strongly absorbs the light at 650-700 nm and 400-500 nm wavelength and reflects the light at 560 nm wavelength. This characteristic is utilized in this research to quantify the pigments amount. Therefore, the leaf digital image was taken individually using Pcopixelfly 14 bit CCD camera with Thorlabs visible bandpass filter (Fig. 1). Ten bandpass filters were used in the experiment i.e. 350, 400, 450, 500, 550, 600, 650, 700, 750 and 800 nm. Each filter will pass the light only in a single wavelength which reflected by the sample leaf being analyzed. Tungsten halogen was used as the light source. It provide a wide range of electromagnetic wavelength from 360-2400 nm.
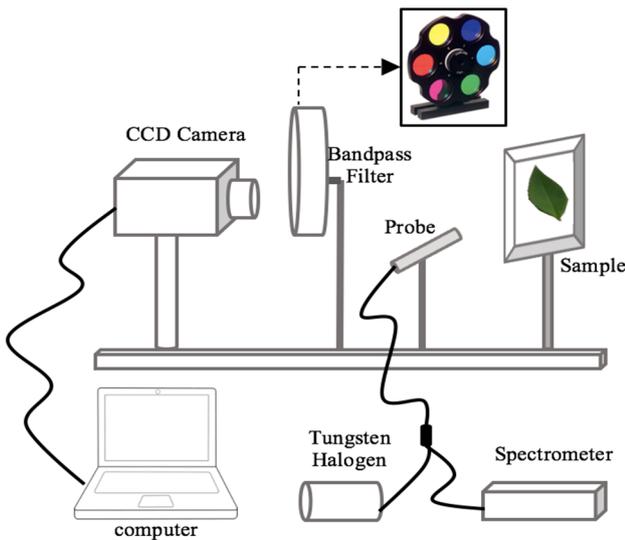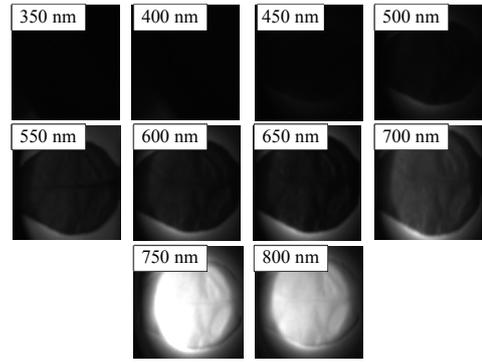

Fig. 1. Data acquisition scheme

Fig. 2. Example of the leaf multispectral image

The results are 10 images (multispectral image) as seen in Fig. 2. An image with bright appearance indicates that the leaf strongly reflects the light and vice versa. As an example, the image labeled 750 nm shown the brightest color, that is mean the sample leaf strongly reflects the light with a 750 nm wavelength. Image preprocessing was conducted to simplify the input such that CNN algorithm could run faster. Two preprocessing procedures were applied to each digital image, i.e., segmentation and resizing. Segmentation was aimed to extract only the leaf area because the ultimate goal of the experiment is to recognize the color variation. Unlike other common CNN implementation which is focused on the shape recognition, in this research shape was not important otherwise color structure was the most valuable feature. Resizing was aimed to reduce the total amount of the pixel that will proceed in the CNN and to equate the overall size of the input image at once. These images were then used as the input of the CNN.

C. Pigment Content Measurement

Chlorophyll, carotenoid, and anthocyanin content were measured using non-destructive spectrometer (Ocean Optic USB-4000). The measurement process was done simultaneously with the digital image acquisition (Fig. 1). A leaf sample is exposed to light from the light generator (tungsten halogen) via a probe. In the same time, the probe captured the reflected light and sending it to the spectrometer. The spectrometer then measures the intensity and send it to the computer for the quantification and visualization. Pigments content was then calculated using (1) and (2) for chlorophyll, (3) and (4) for carotenoid and (5) for anthocyanin [17].

$$(Chl)RI_{green} = \left[\frac{R_{750-800} - R_{430-470}}{R_{520-580} - R_{440-480}} \right] - 1 \tag{1}$$

$$(Chl)RI_{red\ edge} = \left[\frac{R_{750-800} - R_{430-470}}{R_{659-740} - R_{440-480}} \right] - 1 \tag{2}$$

$$CRI_{green} = \left[(R_{510})^{-1} - (R_{550-570})^{-1} \right] * R_{750-800} \tag{3}$$

$$CRI_{red\ edge} = \left[(R_{510})^{-1} - (R_{700-710})^{-1} \right] * R_{750-800} \tag{4}$$

$$ARI = \left[(R_{500-570})^{-1} - (R_{700-710})^{-1} \right] * R_{750-800} \tag{5}$$

(Chl)RI stands for chlorophyll reflectance index, *CRI* is carotenoid reflectance index, and *ARI* is anthocyanin reflectance index. These indices was then used as the output of the CNN representing the pigments content.

D. Dataset Preparation

Table 1 describes the dataset structure. Each leaf digital image will be paired with the 5 pigment indices. From those pairs, 80% will be randomly selected as the training set, and the remaining will be the test set.

TABLE I.   STRUCTURE OF THE DATASET

Digital Image	leaf1.jpg	...	leaf391.jpg
$(Chl)RI_{green}$	0.45	...	0.89
$(Chl)RI_{rededge}$	1.24	...	1.45
CRI_{green}	-0.11	...	0.04
$CRI_{rededge}$	0.84	...	0.03
ARI	0.72	...	0.01

E. Design of the CNN Architecture

Three CNN models was implemented and evaluated in the experiment, i.e., ShallowNet, AlexNet and VGGNet. OpenCV library was used to preprocess the multispectral images. For the ShallowNet and AlexNet architectures, multispectral images were resized to 32x32 pixel, and for the AlexNet architecture, the images were resized to 120x120 pixel. Among those three CNN model, ShallowNet is the simplest model and AlexNet is the most complex model.
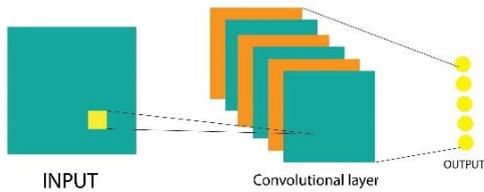

Fig. 3.   ShallowNet architecture

1) ShallowNet: Fig. 3 depicts the architecture of ShallowNet. There was 1 convolution layer with 32 filters in size 3x3 and 1 output layer with 5 nodes. Each node in the output utilizes LeakyRelu activation function and represents the pigment indices.

2) AlexNet: Fig. 4 depicts the architecture of AlexNet. There were 5 convolution layers and 3 fully connected layers. Design of each layer can be seen in Table II.

TABLE II.   DETAIL OF THE ALEXNET ARCHITECTURE

Hidden Layer		Design
Convolution	1	96 filters in size 11x11 with max pooling in size 3x3
	2	256 filters in size 5x5 with max pooling in size 3x3
	3	384 filters in size 3x3 without pooling
	4	384 filters in size 3x3 without pooling
	5	256 filters in size 3x3 with max pooling in size 3x3
Fully Connected	1	4096 nodes with LeakyRelu activation function
	2	4096 nodes with LeakyRelu activation function
	3	1000 nodes with LeakyRelu activation function

3) VGGNet: Fig. 5 depicts the architecture of VGGNet. There were 10 convolution layers and 3 fully connected layers. Design of each layer can be seen in Table III.
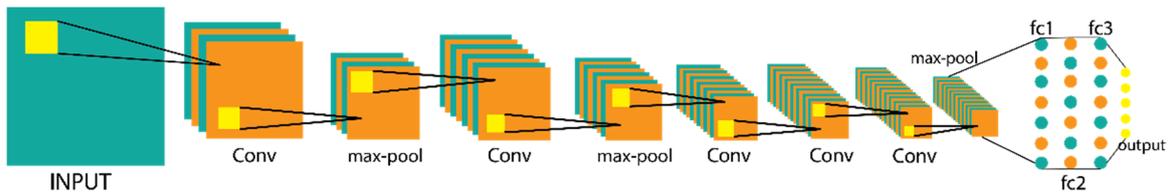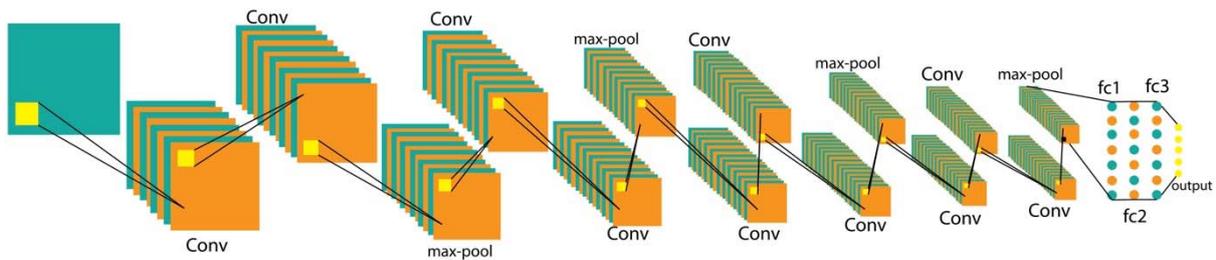

Fig. 4.   AlexNet architecture

Fig. 5.   VGGNet architecture

F. Implementation

Python 3 with Tensorflow library and Keras API was used to develop CNN architecture. The experiment was run on the personal computer with 2.3 GHz Intel Core i5, RAM 8 GB DDR3L, and Windows 10 operating system.

TABLE III.   DETAIL OF THE VGGNET ARCHITECTURE

Hidden Layer		Design
Convolution	1	8 filters in size 2x2 without pooling
	2	8 filters in size 2x2 with max pooling in size 2x2
	3	16 filters in size 2x2 without pooling
	4	16 filters in size 2x2 with max pooling in size 2x2
	5	32 filters in size 2x2 without pooling
	6	32 filters in size 2x2 without pooling
	7	32 filters in size 2x2 with max pooling in size 2x2
	8	64 filters in size 2x2 without pooling
	9	64 filters in size 2x2 without pooling
	10	64 filters in size 2x2 with max pooling in size 2x2
Fully Connected	1	4096 nodes with Relu activation function
	2	4096 nodes with Relu activation function
	3	1000 nodes with Relu activation function
	4	5 nodes with LeakyRelu activation function

G. Optimization Method

The optimization algorithm was used to minimize the error function. This function is dependent on the internal parameters (weights dan bias) such that while minimizing the error, the internal parameters are updated as well. Gradient descent is a fundamental technique used to optimize the error function. However, because of its weaknesses, many researchers have developed variants of this technique. Two of the most recent development of gradient descent variants are Root Mean Square Propagation (RMSProp) [18] and Adaptive Moment Estimation (Adam) [19] which were used in this research. The RMSProp optimizer reduces the error function fluctuation caused by stochastic gradient descent technique. It also determines a learning rate value for each parameter automatically. Each internal parameters (ω) are updated using (6), (7), and (8). Whereas η is initial learning rate, v_t is exponential average of squares of gradients and g_t is gradient of time t along ω^j.

$$v_t = \rho v_{t-1} + (1-\rho).g_t^2 \qquad (6)$$

$$\Delta \omega_t = -\frac{\eta}{\sqrt{v_t+\varepsilon}}.g_t \qquad (7)$$

$$\omega_{t+1} = \omega_t + \Delta \omega_t \qquad (8)$$

Adam optimizer improves the RMSProp technique. Rather than adjusting the learning rate by the average of the first moment (the mean), Adam makes utilization of the average of the second moments of the gradients (the

variance). This approach makes Adam able to achieve good results faster. The internal parameters (ω) are updated using (9), (10), and (11). Whereas m_t is the mean and v_t is the variance of the gradient.

$$m_t = \frac{m_t}{1-\beta_1^t} \qquad (9)$$

$$v_t = \frac{v_t}{1-\beta_2^t} \qquad (10)$$

$$\omega_{t-1} = \omega_t - \frac{\eta}{\sqrt{v_t+\varepsilon}}.m_t \qquad (11)$$

H. Performance Indicator

Unlike other common CNN model which is intended to conduct a classification task, the CNN model in this research was aimed to run a prediction task. Therefore, the classification performance indicator such as accuracy, specificity, and sensitivity was not used to evaluate the model. Otherwise, Mean Square Error (MSE) was applied for the evaluation. The MSE calculation is based on (12), y_i is the actual pigment content (represent by reflectance index), $\hat{y}_i$ is the prediction of the actual pigment content and *n* is the total amount of data.

$$MSE = \frac{1}{n}\sum_{i=1}^{n}(y_i - \hat{y}_i)^2 \qquad (12)$$

III. RESULT AND DISCUSSION

A. Data Collection

Table IV describes the color distribution of the leaf samples. Yellow and yellowish green is the most challenging sample to collect. In the most plants, those colors will appear in the aging stage. Unfortunately, in the aging stage the structure of the leaf has started to damage as well. Therefore, such leaves will cause improper color variation to describe the pigment content. In this research the yellow and yellowish green samples were obtained from the fresh *Piper betle L* leaves, this kind of plant will produce yellow leaves in the normal stage not only in the aging stage. All samples were come from a several healthy plants.

TABLE IV.   SAMPLE DISTRIBUTION

Group of Visual Color	Data Amount
Green	97
Red	90
Yellow	50
Reddish Green	147
Yellowish Green	60

Fig. 6 depicts the pigments content distribution of *Syzygium oleana*. It can be seen that the pigments content of each color category (green, reddish green, and red) confirms the theory that the visual color of leaves could well represent its pigment content. The red leaves seem to have more anthocyanin and less chlorophyll. Otherwise, the green and reddish green leaves seem to have more chlorophyll and less anthocyanin. This data also justify that *Syzygium oleana* is suitable to provide the variation on anthocyanin content data. Table V describes the minimum and maximum value of the pigments content in *Syzygium oleana*.
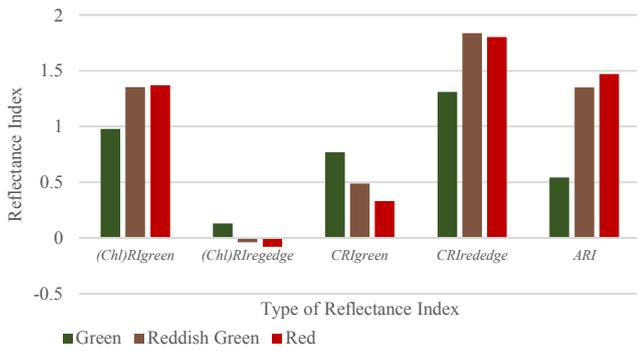
Fig.6. Pigment content distribution of *Syzygium oleana*

TABLE V. THE RANGE OF *SYZYGIUM OLEANA* PIGMENTS CONTENT

Pigment Content Metric	Minimum	Maximum
$(Chl)RI_{green}$	0.407663	1.857813
$(Chl)RI_{red}$	-0.107580	0.323876
CRI_{green}	0.157148	0.981661
CRI_{red}	0.814667	2.226155
ARI	0.283901	1.967888

Fig. 7 depicts the pigments content distribution of *Piper betle L*. As well as on *Syzygium oleana,* the pigments content of each color category (yellowish green and yellow) also confirms the color-pigment content relationship theory. The yellow leaves seem to have more carotenoid and less chlorophyll. All of the leaves seem to have a little amount of anthocyanin. This fact also justifies that *Piper betle L* is suitable to provide the variation on carotenoid content data. Table VI describes the minimum and maximum value of the pigments content in *Piper betle L*.
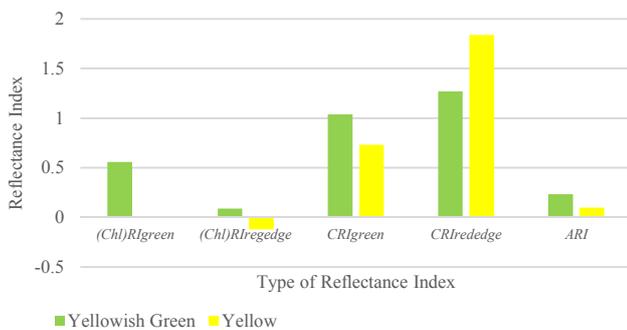

Fig.7. Pigment content distribution of *Piper betle L*

TABLE VI. THE RANGE OF *PIPER BETLE L* PIGMENTS CONTENT

Pigment Content Metric	Minimum	Maximum
$(Chl)RI_{green}$	-0.116920	0.793131
$(Chl)RI_{red}$	-0.161180	0.161759
CRI_{green}	0.442079	1.137226
CRI_{red}	0.511603	1.398290
ARI	0.065826	0.302499

B. Selection of The Best CNN Architecture

Experiments to determine the best CNN architecture were done by making some changes to the CNN parameters, i.e., optimizer type, number of batch size, and number of the epoch. Adaptive Moment Estimation (Adam) and Root Mean Square Propagation (RMSProp) were selected as variations of the optimizer. Batch size was tried with the size of 30, 60, and 120 while the epoch was tested in the number of 15, 30, and 45.

1) ShallowNet: Table VII and VIII summarize the performance of the ShallowNet architecture using MSE as the performance indicator. The lowest MSE (both during training and testing) is obtained while using the Adam optimizer with batch size 30 (see the grayed-out cells). The ideal number of the epoch is 15.

TABLE VII. IN SAMPLE MSE OF SHALLOWNET ARCHITECTURE

Epoch	Batch Size					
	30		60		120	
	Adam	RMSprop	Adam	RMSprop	Adam	RMSprop
15	0.0037	0.0433	0.0373	0.0544	0.0936	0.2938
30	0.0094	0.0086	0.5621	0.0191	0.6551	0.0315
45	0.0047	0.0417	0.4363	0.0164	0.5771	0.0313

TABLE VIII. OUT SAMPLE MSE OF SHALLOWNET ARCHITECTURE

Epoch	Batch Size					
	30		60		120	
	Adam	RMSprop	Adam	RMSprop	Adam	RMSprop
15	0.0060	0.0486	0.0355	0.0661	0.1012	0.2800
30	0.0096	0.0126	0.5380	0.0205	0.6310	0.0330
45	0.0064	0.0417	0.4118	0.0212	0.5531	0.0355

2) AlexNet: Table IX and X summarize the performance of the AlexNet architecture. The same as before, it is using MSE as the performance indicator. The lowest MSE (both during training and testing) is obtained while using the Adam optimizer with batch size 30. The ideal number of the epoch is 45 (see the grayed-out cells). Compared to the ShallowNet architecture, the lowest MSE of AlexNet architectures is still greater than the ShallowNet lowest MSE.

TABLE IX. IN SAMPLE MSE OF ALEXNET ARCHITECTURE

Epoch	Batch Size					
	30		60		120	
	Adam	RMSprop	Adam	RMSprop	Adam	RMSprop
15	0.1753	0.3549	0.0658	0.0795	0.1708	0.3494
30	0.1804	0.0244	0.1699	0.3277	0.1694	0.3162
45	0.0061	0.0178	0.0079	0.0545	0.1695	0.0712

TABLE X.   OUT SAMPLE MSE OF ALEXNET ARCHITECTURE

Epoch	Batch Size					
	30		60		120	
	Adam	RMSprop	Adam	RMSprop	Adam	RMSprop
15	0.1512	0.3316	0.0677	0.0743	0.1463	0.3362
30	0.1563	0.0219	0.1457	0.3000	0.1456	0.2918
45	0.0074	0.0177	0.0087	0.0512	0.1455	0.0674

3) VGGNet: Tables XI and XII summarize the performance of the VGGNet architecture and still using MSE as the performance indicator. The lowest MSE (both during training and testing) is obtained while using the Adam optimizer with batch size 30 (see the grayed-out cells). The ideal number of the epoch is 30. Compared to the ShallowNet and AlexNet architecture, the lowest MSE of VGGNet architectures is still greater than the lowest MSE of the other two CNN models.

TABLE XI.   IN SAMPLE MSE OF VGGNET ARCHITECTURE

Epoch	Batch Size					
	30		60		120	
	Adam	RMSprop	Adam	RMSprop	Adam	RMSprop
15	0.0127	0.0318	0.1269	0.1860	0.1712	0.1404
30	0.0086	0.0174	0.0075	0.1107	0.1692	0.1767
45	0.1696	0.0218	0.1692	0.0281	0.1692	0.1924

TABLE XII.   OUT SAMPLE MSE OF VGGNET ARCHITECTURE

Epoch	Batch Size					
	30		60		120	
	Adam	RMSprop	Adam	RMSprop	Adam	RMSprop
15	0.0145	0.0306	0.1104	0.1761	0.1472	0.1268
30	0.0099	0.0174	0.0085	0.1066	0.1452	0.1582
45	0.1459	0.0227	0.1451	0.0245	0.1452	0.1680

IV. CONCLUSION

The CNN model is proven to be able to find the best color features of leaf multispectral digital images and successfully used it to predict the photosynthetic pigment content. From all experiments with 3 different types of CNN model (ShallowNet, AlexNet, and VGGNet), it was determined that ShallowNet-based architecture be the best architecture for photosynthetic pigment prediction. The architecture reaches lowest MSE while using Adam optimizer and trained with batch size 30 and number of epoch 15 (i.e., 0.0037 for in sample and 0.0060 for out sample). In this case, as the complexity of the CNN architecture is increasing the prediction performance is decreasing. The most straightforward CNN architecture, i.e., ShallowNet was able to model the relationship between visual colors recorded on multispectral digital image and pigments content better than AlexNet and VGGNet.

REFERENCES

[1] S. Sofia, and M.V.M. Teresa, "Quantification of Photosynthetic Pigments of Plants, Water and Sediment Samples in Chirackal and Kattiparambu of Ernakulam District, Kerala," International Journal of Plant & Soil Science, vol.12, no.5, pp.1–7, September 2016.

[2] M.M. Ali, A. Al-Ani, D. Eamus, and D.K.Y Tan, "Leaf Nitrogen Determination Using Non-Destructive Techniques–A Review," Journal of Plant Nutrition, vol.40, no7, March 2017.

[3] S. Sharma, and C. Gupta, "A Review of Plant Recognition Methods and Algorithms," International Journal of Innovative Research in Advanced Engineering, vol. 2, no. 6, pp.111-116, June 2015.

[4] A. Shabani, K.A. Ghaffary, A.R. Sepaskhah, and A.A. Kamgar-Haghighi, "Using the Artificial Neural Network to Estimate Leaf Area," Scientia Horticulturae, vol. 216, pp.103–110, February 2017.

[5] J.D.R. Soares, M. Pasquala, W.S. Lacerdab, S.O. Silvac, and S.L.R. Donatod, "Comparison of Techniques Used in The Prediction of Yield in Banana Plants," Scientia Horticulturae, vol.167, pp. 84–90, March 2014.

[6] M.R.N. Rad, S. Koohkan, H.R. Fanaei, and M.R.P. Rad, "Application of Artificial Neural Networks to Predict the Final Fruit Weight and Random Forest to Select Important Variables in Native Population of Melon (Cucumis melo L.)," Scientia Horticulturae, vol.181, pp.108–112, January 2015.

[7] S.X. Mei, J. Ying-tao, Y. Mei, L. Shao-kun, W. Ke-ru, and W. Chong-tao, "Artificial Neural Network to Predict Leaf Population Chlorophyll Content from Cotton Plant Images," Agricultural Sciences in China, vol. 9, no.1, pp. 38-45, January 2010.

[8] J.I. Arribas, G.V. Sanchez-Ferrero, G. Ruiz-Ruiz, and J. Gomez-Gil, "Leaf Classification in Sunflower Crops by Computer Vision and Neural Networks," Computer and Electronics in Agriculture, vol.78, no.1, pp.9-18, August 2011.

[9] Y.L. Cun, Y. Bengio, and G. Hinton, "Deep Learning," Nature, vol. 521, pp.436-444, 2015.

[10] Z. Cheng, X. Li, and C.C. Loy, "Pedestrian Color Naming via Convolutional Neural Network," in *Proceeding ACCV,* 2016, pp.35-51.

[11] V.O. Yazici, J.V. Weijer, and A. Ramisa, "Color Naming for Multi-Color Fashion Items," in *Proceeding World CIST*, 2018, pp. 64-73.

[12] M. Dyrmann, H. Karstoft, and H.S. Midtiby, "Plant Species Classification using Deep Convolutional Neural Network," Biosystems Engineering, vol.151, pp.72-80, November 2016.

[13] M.M. Ghazi, B. Yanikoglu, and E. Aptoula, "Plant Identification using Deep Neural Networks via Optimization of Transfer Learning Parameters," Neurocomputing, vol. 235, pp.228–235, April 2017.

[14] J.R. Ubbens, and I. Stavness, "Deep Plant Phenomics: A Deep Learning Platform for Complex Plant Phenotyping Tasks," Frontiers in Plant Science vol.8, pp.1190, July 2017.

[15] S.P. Mohanty, D.P. Hughes, and M. Salathé, "Using Deep Learning for Image-Based Plant Disease Detection," Frontier Plant Science, vol.7, pp.1419, September 2016.

[16] A.S. Harrera, "The Biological Pigments in Plant Physiology," Agricultural Sciences, vol.6, pp.1262-1271. October 2015.

[17] A.A. Gitelson, and M.N. Merzlyak, "Non-Destructive Assessment of Chlorophyll, Carotenoid, and Anthocyanin Content in Higher Plant Leaves: Principles and Algorithms," Papers in Natural Resources, vol.263, pp.78-94, 2004.

[18] G. Hinton, N. Srivastava, and K. Swersky. Lecture 6a. Class Lecture, Topic : "Overview of Mini Batch Gradient Descent", Computer Science Department, University of Toronto, 2015.

[19] D.P. Kingma, and J.L. Ba, "Adam: A Method for Stochastic Optimization," in *Proceeding ICLR, 2015.*